

# Petrogenesis of metaluminous and peraluminous granitoids from Garga-Sarali zone : evidence of I- and S-type sources (central African fold belt in Cameroon)

Daama Isaac <sup>1\*</sup>, Mbowou Gbambie Isaac Bertrand <sup>2</sup>, Nguihdama Dagwai <sup>3</sup>, Ngounouno Ismaïla <sup>4</sup>

<sup>1</sup> Department of oil and gas engineering, School of Geology and Mining Engineering, University of Ngaoundere

<sup>2</sup> Department of Mineral prospecting and exploration technologies, School of Geology and Mining Engineering, University of Ngaoundere

<sup>3</sup> Department of Life and Earth Sciences, Ecole Normale Supérieure, University of Maroua

<sup>4</sup> Department of Earth Sciences, Faculty of Science, University of Ngaoundéré

\*Corresponding author E-mail : [idaama.isaac@gmail.com](mailto:idaama.isaac@gmail.com)

## Abstract

The Garga-Sarali granitoids outcrop from a metamorphic basement in the central-eastern part of the Central Cameroonain Domain of the Central African fold belt in Cameroon, and are petrographically very complex. They can be divided into two types : (1) Granodiorites of metaluminous type-I, with a fine-grained porphyritic variant texture, consisting of quartz + orthoclase + microcline + plagioclase + biotite + zircon + oxides ± apatite; (2) and two-mica granites of hyper-aluminous type-S, with a grainy texture, consisting of the same quartz + k-feldspars + biotite + cordierite ± apatite. These formations both belong to a calc-alkaline-subalkaline, hyper-potassic to shoshonitic signature, and to the tectonic domains of volcanic arc granites. Their emplacement is intimately linked to a crustal parent magma (metagrauwackes and metabsalt-tonalites) that imbibed through the openings in the post-orogenic pan-African lithospheric constraints. Their La/Yb ratio, with (La/Sm)<sub>n</sub> ranging from 2.18-5.75 ppm, reflects their richness in LREE, and the average Eu/Eu\* = 0.666 ppm suggests that the residual magma was supersaturated with silica.

**Keywords:** Petrography; Petrogenesis; Granodiorites; Two-Mica Granites; Garga-Sarali.

## 1. Introduction

The Garga-Sarali granitoids belong to the Pan-African Central African Chain (Central African fold belt) and outcrop in slabs and multi-varied blocks (fig. 1). Previous researchs carried out in this area, such as the Magnetic Susceptibility Anisotropy (MSA) (Kankeu et al., 2006) and the geochemistry study of the Garga-Sarali granitoids (Daama et al., 2020), were not focused on the petrogenesis of these formations. The aim of this study is to provide a detailed petrographic and petrogenetic description of these granitoids, in order to contribute to improving and extending the knowledge available on the plutonic formations of the Pan-African Central African Chain.

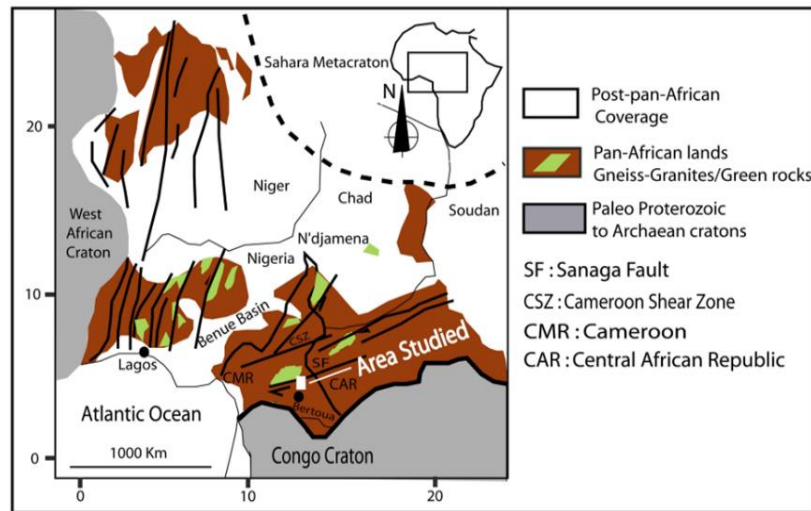


Fig. 1: Post Pan-African and Pan-African in Central Africa, (After Ferré Et Al., 1996 ; Toteu Et Al., 2004).

## 2. Geological setting

The studied area consists mainly of migmatites and gneisses (Ndokayo orthogneiss), schists of the presumed Lom schist belt, meta-leucogranites, metagranodiorites, porphyroid granites and fine-grained Kongolo granites (Kankeu et al., 2006). The porphyritic and fine-grained granites contain schist enclaves (Daama et al., 2020) that display crenulation schistosity and folds. These structural features are controlled by the Sanaga ENE-WSW-trending fault (Ngako et al., 1991). A major antiform has been indicated, parallel to the Sanaga fault. These structures are intimately linked and interpreted as the products of transpression (Kankeu et al, 2009). Late-tectonic granites (including those of Garga-Sarali) are emplaced during strike-slip deformation, characterised by subhorizontal lineations that reflect the magma factory.

## 3. Methodology and analytical methods

26 thin sections were carried out in the laboratory of the “Institut de Recherches Géologiques et Minières (IRGM)” in Yaoundé. The computer-assisted microscope was used in the Mineral Processing Laboratory (LTM) at IRGM to identify and describe the various parageneses. The analytical methods of ICP-ES and ICP-MS were used at Veritas laboratory in Vancouver (Canada), to perform representative analysis of major and trace elements on seventeen samples. Thus, this geochemical analysis was done using the pulp. Whole-rock analyses were done by Inductively Coupled Plasma-Atomic Emission (ICP-AES) for major elements and by Inductively Coupled Plasma Mass Spectrometry (ICP-MS) for trace elements. The samples were pulverized to obtain a homogeneous sample, out of which 50–60 g were obtained for the analyses. 0.1 g of rock powder was fused with 1.5 g of  $\text{LiBO}_2$  and then dissolved in 100 mm<sup>3</sup> of 5%  $\text{HNO}_3$ . Loss on ignition (LOI) was determined by the weight difference after ignition at 1025 °C. Some samples were crushed to extract cordierite megacrysts (figure 2). Various standards were used, and data quality assurance was verified by running these standards between samples as unknowns.

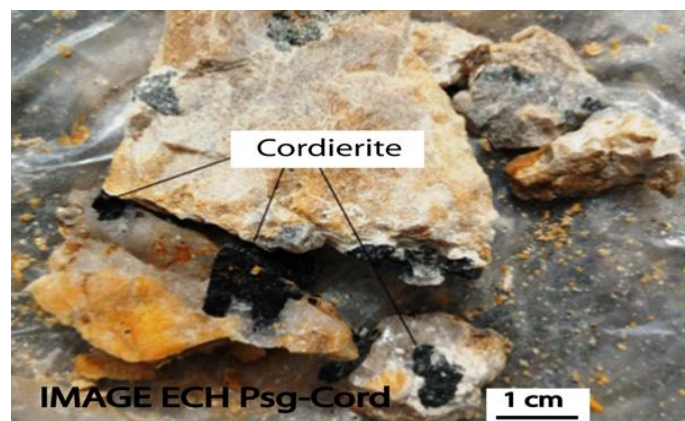


Fig. 2: Cordierite Megacrystals in Two Mica Granites.

## 4. Petrography

The Garga-Sarali granitoids outcrop from a gneissic and schist basement (fig.6) and can be classified into two main types: granodiorites and two-mica granites crossed by cordierite pegmatites. Granodiorites and two-mica granites belong respectively to metaluminous and peraluminous domain.

#### 4.1. Granodiorites (metaluminous granitoids)

Granodiorites are found precisely in Ndanga-Gadima, Kongolo and western edge of Kongolo sectors.

- The Ndanga-Gadima (NG) type, (05°25'51"N; 14°02'27"E) outcrops in blocks (~5 m), slabs (~25 m) of medium-grained texture, they are whitish, mottled black, slightly altered, containing double schist enclaves. They consist of sub-hedral quartz (0.3—1.3mm, 20 vol.%), more or less embedded in feldspars and oxides; orthoclase (1—4mm, 15 vol.%), tabular and prismatic; compact spathic microcline (>3mm, 30%) with polysynthetic macle. Sub-hedral plagioclases, (>5mm, < 10 vol.%) with sharp rectilinear contours are present; Biotite (0.5-4 mm, 10 vol.%) crystals are skeletal lamellae. Zircon is rare (<2%, <1mm) and occurs as a prismatic-rounded inclusion in quartz. Apatite is very small (<5 vol.%, <1µm), sub-hedral, and oxides (~ 8 vol.%) are seen as inclusions in K-feldspars.
- The Kongolo type, with a micro-grained texture (< 2 mm), outcrops (a, b), (05°23'33" N; 14°01'26"E), in blocks (≤5 m) and slabs (≤ 22 m). Its paragenesis differs from that of the Ndanga-Gadima type by the absence of apatite and plagioclase crystals.
- The porphyroid type on the western edge of Kongolo (05°22'50"N; 13°59'29"E) outcrops in the form of very large boulders (< 1 m) and slabs (12—30 m size). Their porphyritic texture consists of abundant orthoclase (<4mm, 45 vol.%), quartz (<2mm, 15—20 vol.%), biotite (30 vol.%), and oxides included in the quartzo-feldspathic matrix.



**Fig. 3:** Macroscopic and Microscopic Photographs of Granodiorites (Qtz = Quartz, Orth = Orthoclase, Mcr = Microcline, Pl = Plagioclase, Bt = Biotite, Zr = Zircon, Apt = Apatite, Ox = Oxide).

#### 4.2. Two-mica granites (peraluminous granitoids)

Two-mica granites outcrop (05°19'34"N; 14°02'50"E) in form of blocks (~2 m), and slabs (~30 m) containing cordierite grains (fig. 4. h). These granites are crossed by cordierite-bearing pegmatites and have a slightly weathered appearance (fig. 4. f) with a grainy texture (fig. 4. g).

Its petrographic component consists with: sub-hedral quartz (0.3-1.3 mm, 20 vol.%) (fig. 4. b); prismatic orthoclase (2—6 mm, 25 vol.%) with traces of destabilization (fig. 4. c); subhedral microcline (>2mm, 10%), tabular, mottled, with an observable aspect of alteration (fig. 4. a); Muscovite forms huge large euhedral laminae (> 0.5 mm, 20 vol.%) and open cleavages filled with oxides and alkali feldspars. Biotite (0.2—3 mm, 10 vol.%) occurs in very elongated aggregates rich in oxide inclusions. Sub-hedral plagioclase (>1mm, vol. 5 vol.%), jointed with orthoclase and biotite, and showing polysynthetic macles (fig. 4. e, f); Cordierite (> 3 mm, 7 vol.%) are present in pseudo-hexagonal crystals (fig. 4. c, d). Apatite is tabular tending to hexagonal form (≤ 0.5mm, 3 vol.%); Oxides (≤ 0.3mm, 5 vol.%) are present.

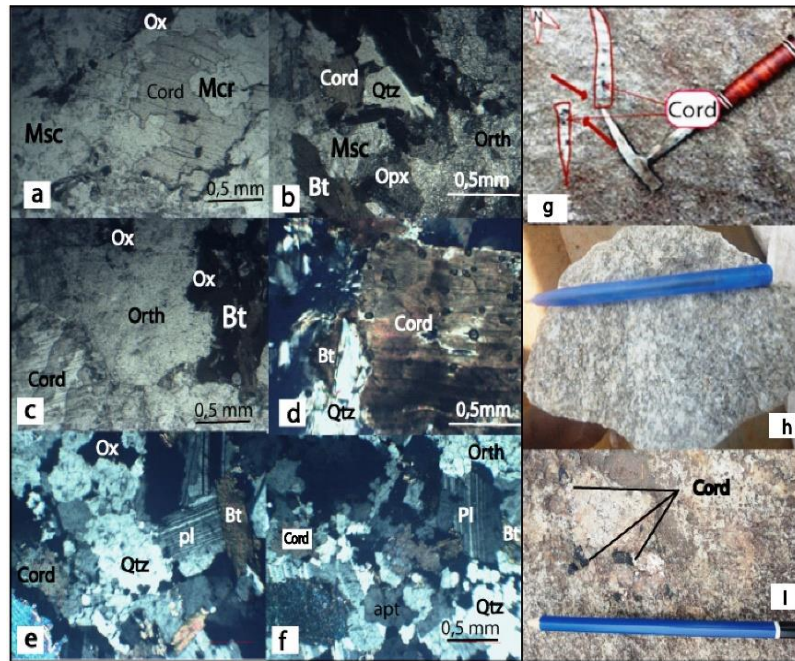


**Fig. 4:** Macroscopic and Microscopic Photographs of Two-Mica Granites. (Qtz = Quartz, Orth = Orthoclase, Mcr = Microcline, Pl = Plagioclase, Bt = Biotite, Apt = Apatite, Cord = Cordierite, Ox = Oxide).

### 4.3. Cordierite-bearing pegmatite

Cordierite-bearing pegmatites of Garga-Sarali oriented N65—80°E, are characterised by its texture and the occurrence of Quartz + Feldspar + Biotite + Muscovite + Cordierite (fig. 5. b, c, d (fig. 5. e, f). Crystals of quartz, feldspars, muscovite and biotite are subhedral and vary in size from 0.5 cm to 2 cm. Cordierite occurs as independent grains scattered in the pegmatitic matrix, usually in a certain alignment (fig. 5. a, e).

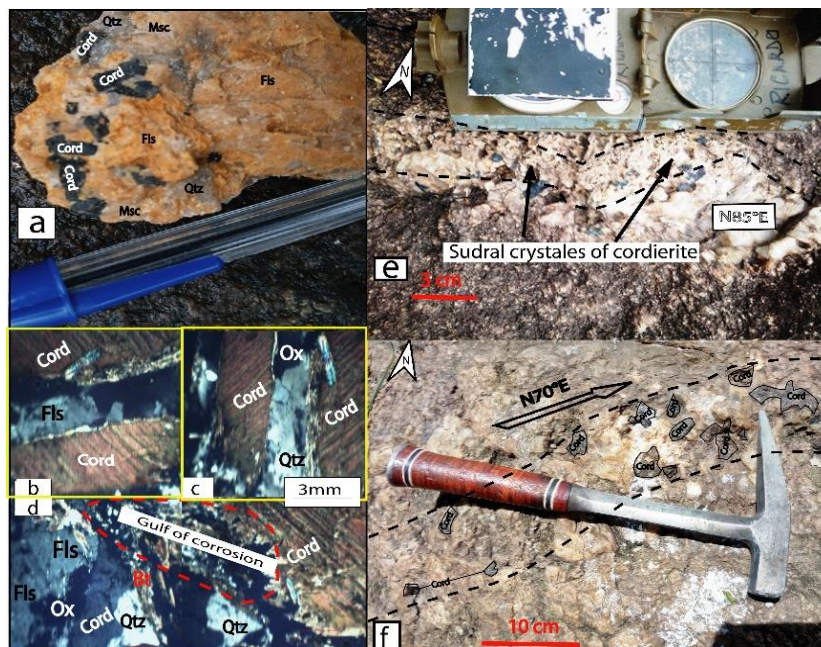


**Fig. 5:** Cordierite-Bearing Pegmatite.

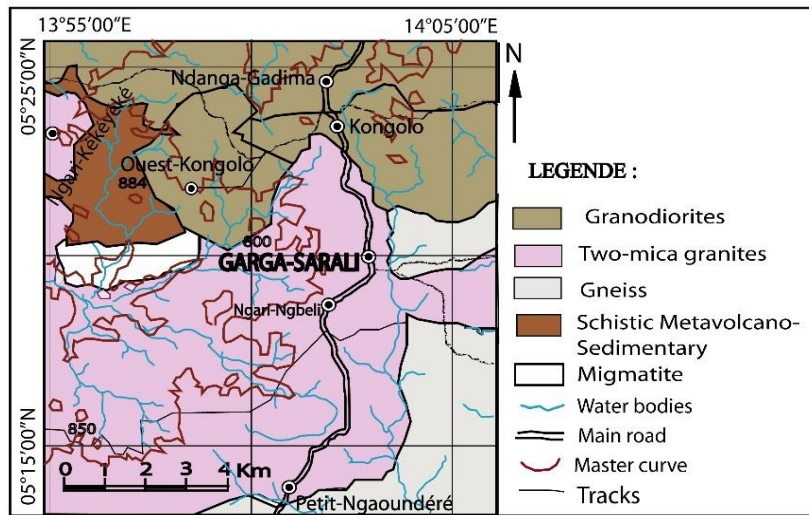


Fig. 6: Geological Map of the Studied Area of Garga Sarali.

## 5. Geochemical data and petrogenetic implications

### 5.1. Nomenclature of the studied rocks

All the Ndanga-Gadima, Kongolo and western Kongolo samples belong to a typically granodioritic end of the calc-alkaline series (Fig. 7.a), and those from the Garga-Sarali two-mica granites fall within the granite series. Discrimination of  $10000\text{Ga}/\text{Al}$  as a function of Zr shows that all these samples fall within the field of type I & S granites.

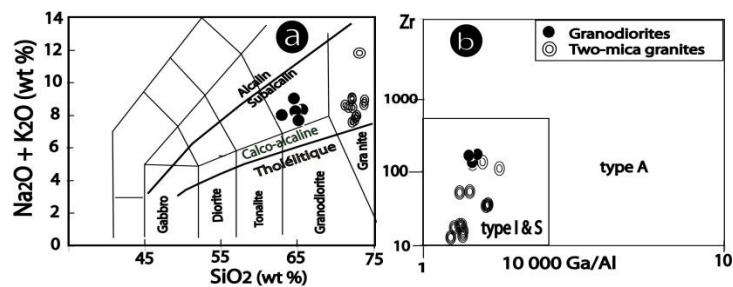


Fig. 7: Total Alkalinity Diagram (TAS) By Macdonald and Katsura (1964) (A); And Discrimination Diagram for Type A and Type I & S Granites by (Whalen Et Al., 1987) (B).

### 5.2. Nature of the magma source

Type-I granodiorites with metaluminous signature (fig. 8.a) are thought to have resulted from subcrustal partial melting of a mainly metabasalt-tonalite (fig. 8.b). Type-S peraluminous granite with two micas (fig. 8. a) is thought to have resulted from supra-crustal partial melting of an essentially metagrawackes compound (fig. 8. b).

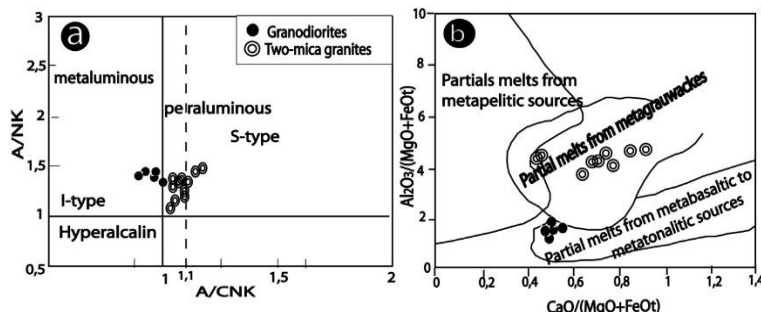
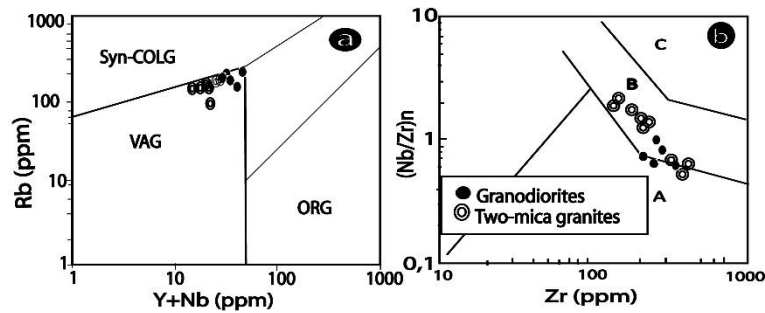


Fig. 8: A/CNK vs A/NK Diagram According to (Shand Et Al., 1943), and  $\text{CaO}/(\text{Mgo}+\text{Feot})$  vs  $\text{Al}_2\text{O}_3/(\text{Mgo}+\text{Feot})$  According to the Dehydration Experiment of (Wolf and Wyllie, 1994).

### 5.3. Tectonic field setting

The Tecto-discriminant of Rb (ppm) versus Y+Nb (fig. 9. a), shows the exclusive positioning of all the samples in the field of volcanic arc granites (VAG). The diagram (fig. 9. b) of Nb/Zr (normalised to the primitive mantle (McDonough and Sun, 1995) as a function of Zr (b) shows that all the samples are located in the field of collisional rocks.



**Fig. 9:** Tecto-Discrimination of Rb as A Function of (Y + Nb) (A) (Pearce Et Al., 1984); and Diagram of (Nb/Zr)/n as A Function of Zr (Thiéblemont Et Al., 1994) (B). A = Subduction Zone Magmatism Rocks; B = Collision Zone Rocks; C = Intraplate, Alkaline Rock; WPG = Intraplate Domain Granites; VAG = Volcanic Arc Granites; Syn-COLG = Syn-Collisional Granite; ORG: Oceanic Rift Granites.

#### 5.4. Alkaline behaviour

The diagrams of figure 10 show that all the samples from granodiorites are trans-alkaline, i.e. sub-alkaline (a), and belong to the shoshonitic series (b), whereas those from two-mica granites split between the trans-alkaline and calco-alkaline field (a), and are hyper-potassic to shoshonitic (b).

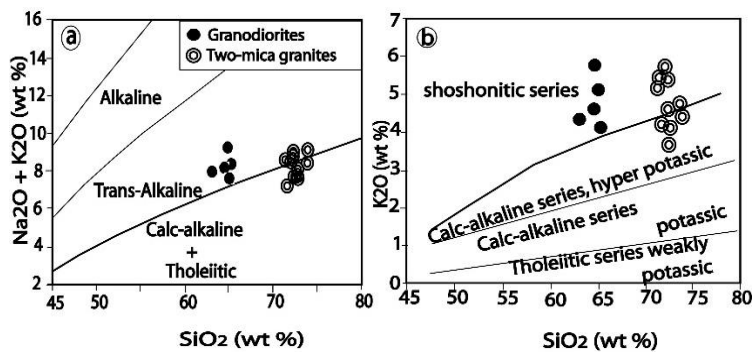


**Fig. 10:** Na<sub>2</sub>O+K<sub>2</sub>O Versus SiO<sub>2</sub> Diagram from Middlemost (1997) (A); and K<sub>2</sub>O Versus SiO<sub>2</sub> Evolution Diagram (Maître Et Al., 1989).

## 6. Discussion

### 6.1. Occurrence model of studied rocks

The size of the outcrops, which for the most part is decametric, is explained by the width of the lithospheric fissures left by the multiple faults during a major phase of pan-African cooling, according to the model in figure 11. The frank contact of these granites with the metamorphic host rock is evidence of a high temperature contrast, which would not have allowed the assimilation of the edge

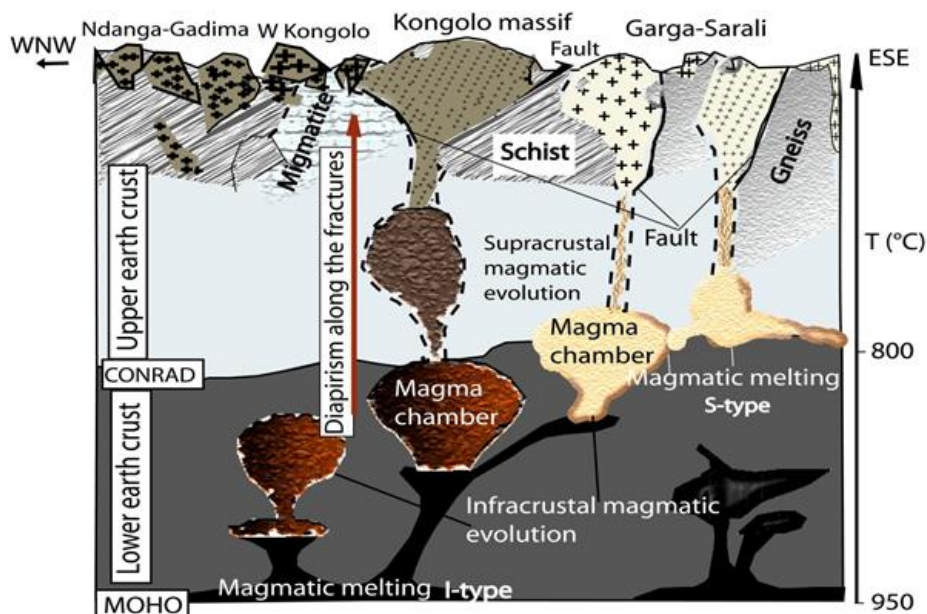


**Fig. 11:** Emplacement of Outcrops (Boulders, Slabs, Plutons) of the Garga-Sarali Granitoids Beside A Gneissic and Schist Basement (Modified After Haimeur Et Al., 2004).

## 6.2. Geodynamic context

The total alkali diagram (fig. 12a) indicates that the studied samples are granodiorites and granites from calc-alkaline setting, typically similar to other granitoids of the Pan-African litho-structural domain (Toteu et al., 2004), in particular the granitoids of the Mbip Tcholliré massif (Nomo et al., 2017) which share the same tectonic context (fig.12. a). And especially those of Mbaibokoum (Naimou et al., 2014), which have a virtually identical calc-alkaline footprint (fig.12. b). This suggests magmatic proximity to a subducted crust, where products such as metagrauwackes would have undergone dehydration according to the experiments of Shand et al. (1943), leading to the formation of the S-type granites similar to those from Garga-Sarali.

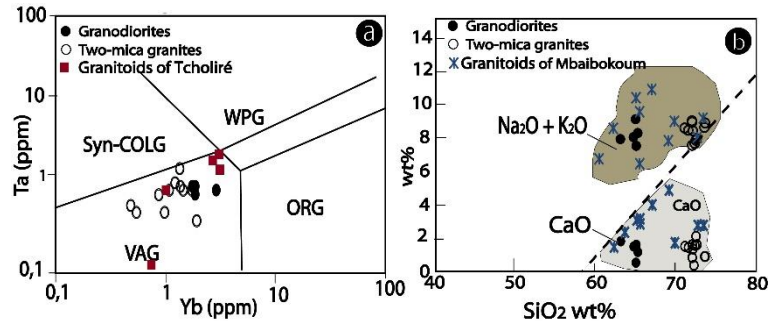


**Fig. 12:** Tectonic-Discriminant Diagram Yb vs Ta (Pearce Et Al., 1984), and SiO<sub>2</sub> vs (Na<sub>2</sub>O+K<sub>2</sub>O) and CaO Correlating Samples from the Granitoids of Garga-Sarali and Surrounding Compared to Those from the Mbip Massif of Tcholliré (Nomo Et Al., 2017) (A). and Diagram of Correlating Samples of Granites from Garga-Sarali and Environs, with Those from Mbaibokoum (Naimou Et Al., 2014) (B).

## 6.3. Inferences concerning crystallisation

Figure 13 shows the evolution of the major and trace elements in the samples as a function of SiO<sub>2</sub> (Harker, 1909). Ferromagnesium (Fe<sub>2</sub>O<sub>3</sub>, MgO), CaO, TiO<sub>2</sub>, MnO and P<sub>2</sub>O<sub>5</sub> show decreasing trends, which are respectively compatible with fractional of biotite, plagioclase, oxides and apatite crystals. The evolution of Al<sub>2</sub>O<sub>3</sub> shows sub-vertical decreases in their content during the differentiation of the samples, which would be in the distinctive agreement with fractional crystallisation of aluminous minerals such as muscovite and cordierite, and that of K<sub>2</sub>O bears witness to the growth of potassic feldspars (orthose, microcline) in the migmatitic liquid. Trace elements also show similar patterns of decrease to those of the major elements, with the exception of Ta, which is a highly incompatible element that shows an increasing trend during the differentiation of these rocks. The very marked fall in zirconium could explain the crystallisation of zircon observed in the Granodiorites.

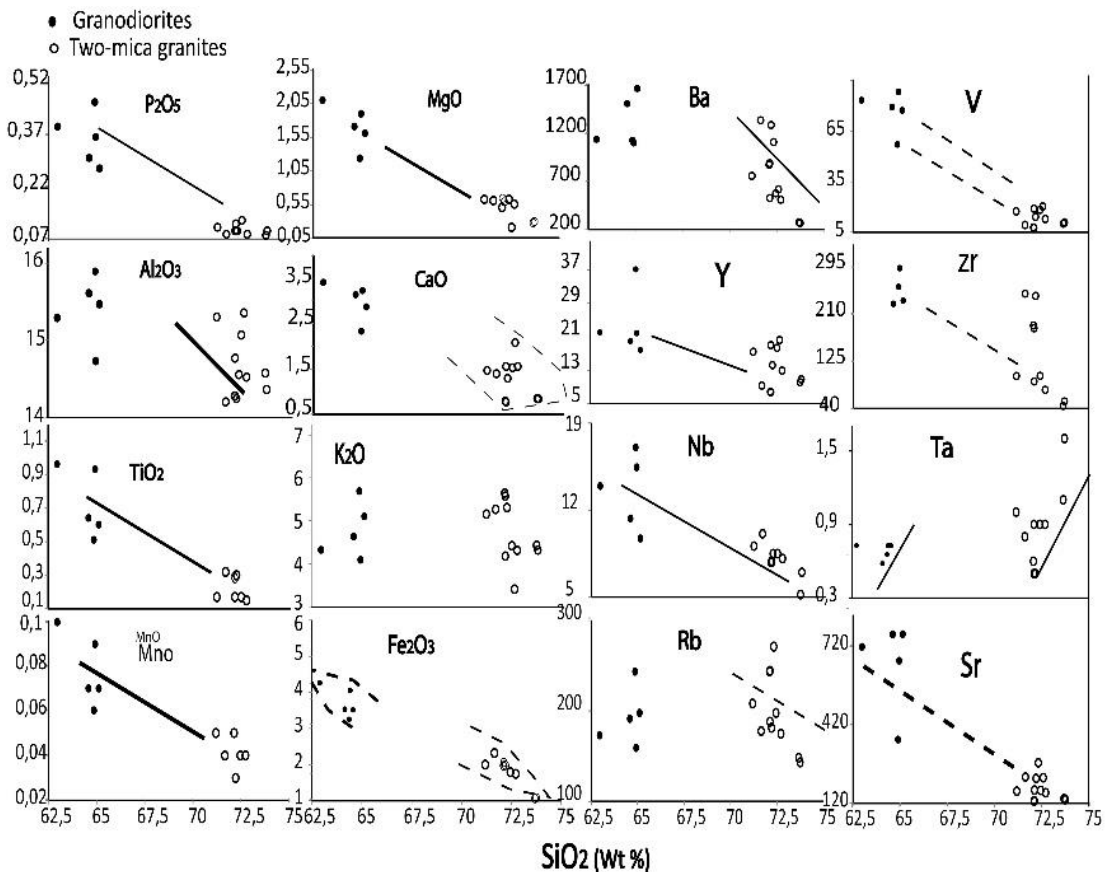


**Fig. 14:** Harker Diagram (1909) of Certain Major and Trace Elements as A Function of Silica (SiO<sub>2</sub>).

Cordierite is frequently found in metamorphic rocks, and its presence in these two-mica granites is highly suggestive of the magmatic materials and particular mechanisms that controlled its formation. According to the dehydration experiment of Wolf and Wyllie, (1994), these rocks were derived from a metagrawacke protolith (fig. 8b). As it happens, the latter is a rock derived from the earlier prograde metamorphism of micaceous and plagioclastic sandstones (Nédélec and Bouchez, 2011), which is a prerequisite that supports the presence of an aluminous mineral such as cordierite in these formations. In addition the work of Vielzeuf and Montel, (1994) on the incongruent melting of metagrawacke at temperature  $750 \leq T^{\circ}\text{C} \leq 1000$  and  $P^{\circ} \leq 800\text{MPa}$ , calibrates that the reaction  $\text{biotite} + \text{quartz} + \text{sillimanite} \pm \text{plagioclase} = \text{granitic liquid} + \text{cordierite}$  at  $P^{\circ} \leq 500\text{MPa}$ . This relationship shows that all the ingredients were present for the cordierite to fractionate in the magmatic liquid, and not to have come from elsewhere (from the host rock as an enclave). Its subhedral crystalline form reinforcing this idea.

However, its absence in biotite granodiorites is not without surprise, since it is thought to be the result of the partial melting of metabasalt-tonalites (see fig. 8), which are poor in aluminous compounds and richer in ferromagnesian. Their ratio  $A/\text{CNK} < 1$  shows that they are metaluminous type-I (fig. 8a), and their ratio  $A/\text{NK} < 1$  fundamentally distinguishes them from silica-rich hyper-alkaline type A granites (fig. 7b) (Loiselle and Wones, 1979). Two-mica granites, on the other hand, are of Type-S, showing high alumina saturation ( $A/\text{CNK} > 1$ ) linked to the presence of S aluminium-hungry minerals (Chapell and White 1974), mainly cordierite. We can also assume that its parent magma was of relatively low temperature and hydrated (Shand et al., 1943), which would have further amplified this alumina enrichment. According to Jonin (1981), cordierite granitoids, because they are hot and dry, have a higher ascent capacity than muscovite-only granitoids, which are cold and wet, which may explain their higher rate of crystallisation at the outcrop surface in our case (see fig 4. i, g; fig 5. e, f).

#### 6.4. REE reports

The variation in the La/Yb ratio shows a scattered and progressive decrease with increasing SiO<sub>2</sub> values (fig. 18.a). The disparity of the samples around the decreasing bilinear ( $\tau$ ) would suggest a re-equilibration of these minerals with residual magmatic fluid. Their high content of heavy rare earths (Daama et al., 2020) could be due to the presence of this fluid at the time of crystallisation, which would have led to vein pockets in the cordierite-bearing pegmatites. The diagram,  $\text{Eu}/\text{Eu}^* = (0.666)$  on average vs SiO<sub>2</sub> has a sub-vertical increasing trend, which would testify to the overgrowth of feldspars in the magmatic fluid, hence perhaps the evidence of abundance of feldspars in these rocks. While for advanced hyper-silicic rocks such as rhyolite, the values (0.65—0.24) in this ratio would explain the supersaturation of the silicic magmatic residue (Mbowou et al., 2012), those in our case (granitic rocks) would confirm this hypothesis. The decrease in the  $\text{Eu}/\text{Eu}^*$  ratio as a function of SiO<sub>2</sub> clearly reflects this supersaturation of the silicic residual magma. This would logically be accompanied by a decrease in the  $\text{Eu}^{3+}/\text{Eu}^{2+}$  ratio, as we move from an oxidising environment to a silicic environment.

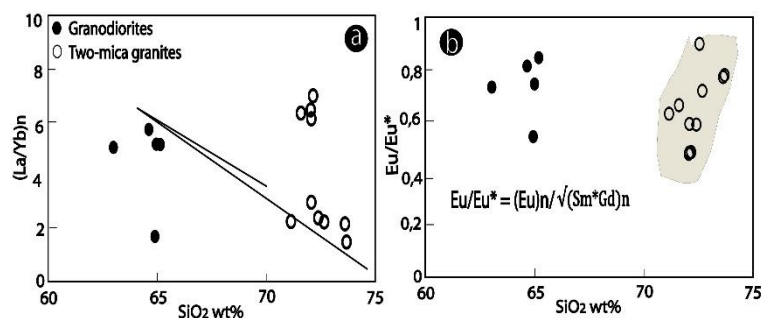


Fig. 14: Diagram of Variations in the La/Yb Ratio (A) and the  $\text{Eu}^*/\text{Eu}$  Ratio (B) as A Function of SiO<sub>2</sub>

## 7. Conclusion

Our study of the granitoids of Garga-Sarali and the surrounding area has led to a number of interpretations and discussions aimed at understanding the petro-magmatic mechanisms that have contributed to their specific characteristics. These formations are of two types, granodiorites and two-mica granites. Their chemical nature is calc-alkaline and they are of type-I and type-S respectively. Their emplacement is thought to be linked to a crustal magma that imbibed through the openings in the pan-African post-orogenic lithospheric constraints. Correlational studies of the Garga-Sarali granitoids have shown a high degree of petrogenetic concordance with certain granitoids of the Central Pan-African African Chain (CPAC). Hyper-aluminous granites often show affinities for the mineralisation of certain rare metals (Nédélec and Bouchez, 2010), so it would be judicious for this work to continue with mineralogical analysis of these formations.

## References

- [1] Kankeu, B., Greiling, R., O., (2006). Magnetic fabrics (AMS) and transpression in the Neoproterozoic basement of Eastern Cameroon (Garga-Sarali area). *Neues Jahrbuch Geologie Paläontologie Abhandlungen* 239, <https://doi.org/10.1127/njgpa/239/2006/263>.
- [2] Daama I., Mbowou Gbambie I., B., Yamgouot Ngounouno F., Ntounde Mama, Ngounouno I., (2020). Geochemistry of Garga-Sarali intrusive granitoids (central domain of the central African fold belt in Cameroon): petrological implication. *International Journal of Advanced Geosciences*. June 2020, 8 (1) (2020) 33-40. <https://doi.org/10.14419/ijag.v8i1.30559>.
- [3] Ferre, E., Gleizes, G., and Caby, R., (2002). Obliquely convergent tectonics and granite emplacement in the trans-Saharan belt of Eastern Nigeria: a synthesis. *Precambrian Res.* 114, 199-219. [https://doi.org/10.1016/S0301-9268\(01\)00226-1](https://doi.org/10.1016/S0301-9268(01)00226-1).
- [4] Toteu, S., F., Penaye, J., and Poudjom, D., Y., (2004). Geodynamic evolution of the pan-African Belt in Central Africa with special reference to Cameroon. *Canadian Journal of Earth Sciences* 41, 73-85. <https://doi.org/10.1139/e03-079>.
- [5] Ngako, V., Jegouzo, p., and Nzenti J., P., (1991). Le Cisaillement Centre Camerounais: rôle structural et géodynamique dans l'orogénèse panafricaine. *C.R. Académie des sciences paris* 313, 457-463. <https://scirp.org/reference/referencespapers?referenceid=2077433>
- [6] Kankeu, B., Greiling, R. O., and Nzenti, J., P., (2009). Pan-African strike-slip tectonics in eastern Cameroon-Magnetic fabrics (AMS) and structure in the Lom basin and its gneissic basement. *Precambrian Research* 17, 258-272. <https://doi.org/10.1016/j.precamres.2009.08.001>.

- [7] MacDonald G.A. & Katsura T. (1964)-Chemical composition of Hawaiian lavas. *J. petrol.*, 25,713-765. <https://doi.org/10.1093/petrology/5.1.82>.
- [8] Whalen J.B., Currie K.L. & Chappell B.W. (1987)- A-types granites: geochemical characteristics, discrimination and petrogenesis. *Contrib. Mineral. Petrol.*, 95, 407-419. <https://doi.org/10.1007/BF00402202>.
- [9] Shand, S., J., (1943). Eruptives rocks : their genesis, composition, classification, and their relations to ore-deposits. *New York*, 444p.
- [10] Wolf M. B., and Wyllie J. P., (1994) Dehydration Melting of Amphibolite at 10 Kbar: The Effects of Temperature and Time. *Contribution to Mineralogy and Petrology*, 115, 369-383. <https://doi.org/10.1007/BF00320972>.
- [11] McDonough, W., F., and Sun, S., S., (1995). The Composition of the Earth. *Chemical Geology*, 120, 223-253. [https://doi.org/10.1016/0009-2541\(94\)00140-4](https://doi.org/10.1016/0009-2541(94)00140-4).
- [12] Thiéblemont, D. and Tegye, M., (1994) Une discrimination géochimique des Roches différenciées témoin de la diversité d'origine et de situation Tectonique des magmas calco-alcalins. *Comptes Rendus de l'Académie Des Sciences*, 319, 87-94. <https://www.scrip.org/reference/referencespapers?referenceid=1535926>
- [13] Pearce, J., A., Harris, N., B., W., and Tindle, A., G., (1984). Trace Element Discrimination Diagrams for the Tectonic Interpretation of Granitic Rocks. *Journal of Petrology*, 25, 956-983. <https://doi.org/10.1093/petrology/25.4.956>.
- [14] Middlemost EAK (1997) Magmas, Rocks, and Planetary Development. Longman Harlow. 10.4236/ijaa.2011.12009
- [15] Le Maître, R., W., Bateman, P., Dudek, A., Keller, J., Lameyre, M., Le Bas, M., J., Sabine, P.A., Schmid, R., Sørensen, H., Streckeisen, A., Woolley, A., R., and Zanettin, B., (1989). A Classification of Igneous Rocks and a Glossary of Terms. Recommendations of the International Union of Geological Sciences Subcommission on the Systematics of Igneous Rocks. *Blackwell Scientific Publications, Oxford*. p.193. <https://www.researchgate.net/publication/234448684>
- [16] Haïmeur, J., El Amrani El Hassani, I-E., et Chabane, A., (2004). Pétrologie et géochimie des granitoïdes calco-alcalins de Zaër (Maroc central) : modèle pétrogénétique. *Bulletin de l'Institut Scientifique, Rabat, section Sciences de la Terre*, n° 2004, n°26, 27-48. 10.4236/nr.2015.611050
- [17] Nomo, N., E., Tchameni, R., Vanderhaeghe O., N., Barbey P., Fosso, P., and Wambo J., (2017). Petrography and Geochemistry of the Mbip Granitic Massif, SW Tcholliré (Central North Cameroon): Petrogenetic and Geodynamic Implication. *International Journal of Geosciences*, 6, 761-775. 10.4236/ijg.2015.67062
- [18] Naimou, S., Alexandre, Ganwa, A., A., Klötzli, U., Kepnamou, A., D., and Emmanuel, E., G., (2014). Petrography and Geochemistry of Precambrian Basement Straddling the Cameroon-Chad Border: The Touboro Baïbokoum Area. *International Journal of Geosciences*, 5, 418-431. <https://doi.org/10.4236/ijg.2014.54040>.
- [19] Harker, A., (1909). The natural history of igneous rocks. New York : Macmillan. <https://www.biblio.com/book/natural-history-igneous-rocks-harker-alfred/d/1424714331>. <https://doi.org/10.2307/1777000>.
- [20] Nédélec, A., and Bouchez, J., L., (2011). Pétrologie des granites. Vuibert and Société géologique de France Editors, 306 p. See discussions, stats, and author profiles for this publication at: <https://www.researchgate.net/publication/317012801>
- [21] Vielzeuf D. & Montel J.M. (1994) – Partial melting of metagrawackes : fluid-absent experiments and phase relationships. *Contrib. Mineral. Petrol.*, 117, 375-393. <https://doi.org/10.1007/BF00307272>.
- [22] Chappell, B., W., et White, A., J., R., (1974). Two contrasting granites types. *Pacific Geology*, 8 : 173-174. 10.4236/gep.2021.910002
- [23] Loiselle M.C Wones D.R. (1979) – Characteristics and origin of anorogenic granites. *Geol. Soc. Am. Abstracts*, 11, 468. 10.4236/jss.2015.34012
- [24] Jonin, M., (1981). Un batholite fini-précambrien : Le batholite mancellien (massif armoricain, France). *Thèse, Brest* : 320P. [https://www.persee.fr/doc/sgeol\\_0302-2692\\_1991\\_num\\_44\\_1\\_1865](https://www.persee.fr/doc/sgeol_0302-2692_1991_num_44_1_1865)
- [25] Eby, G., N. (1990) - the A-type granitoids: a review of their occurrence and chemical characteristics and speculations on their petrogenesis: <https://www.sciencedirect.com/science/article/abs/pii/002449379090043Z>.
- [26] Mbowou, G., I., B., Lagmet, C., Nomadé, S., Ngounouno, I., Déruelle, B., Ohnenstetter, D. (2012) – Petrology of the late cretaceous peralkaline rhyolites (pantellerite and comendite) from lake Chad, Central Africa. *Journal of Geoscience*, 57 (2012), <https://doi.org/10.3190/jgeosci.118>.
- [27] Oukemini Driss, Géochimie, géochronologie (U-Pb) du pluton d'Aouli et comparaisons géochimiques avec d'autres granitoïdes hercyniens du Maroc par analyse discriminante. Thèse de Doctorat en ressources minérales. Décembre 1993, 141 P. <https://doi.org/10.1522/1498481>.